

Optimal path generation for wheeled mobile robots with η^3 -splines

Corrado GUARINO LO BIANCO and Oscar GERELLI

Abstract—This paper deals with the generation of optimal paths planned by means of η^3 -splines, a recently devised planning primitive used for the automated steering of wheeled mobile robots. The shape of η^3 -splines can be easily modified by acting on a set of free parameters. This capability can be used, for example, to satisfy an assigned optimality criterion. In this paper it will be used to minimize the curvature variability in order to reduce the lateral solicitations affecting an autonomous robot. Evidently, curvature derivative could be minimized by means of an optimization algorithm. However, this approach cannot be suitably used in an online application which continuously requires the curve updating. For this reason, closed form expressions have been devised and proposed in this paper in order to efficiently evaluate optimal curves on the sole basis of the interpolating conditions. As a further characteristic, the proposed heuristic method permits obtaining, when appropriate interpolating conditions are given, η^3 -splines which at the best emulate circular arcs and clothoids.

Index Terms—Mobile robots, optimal path generation, geometric continuity.

I. INTRODUCTION

Several approaches can be found in the literature in order to generate appropriate paths for autonomous vehicles. Two different frameworks are normally considered. In the first one, usually indicated with the name of “motion planning”, a structured and known environment is considered. A path joining two given points is generated taking into account the obstacle avoidance problem and possibly satisfying given constraints. A typical constraint is represented by maximum path curvature. The first work related to motion planning was due to Dubin [1]: a minimum length path was generated by means of linear segments and circular arcs. Successively, many other works addressed the same problem [2]–[4]. Recently the problem has been enriched by considering the generation of continuous curvature paths [5].

In the second framework, usually indicated with the term of “motion generation”, the planing phase assumes local characteristics being focused on the generation of short distance paths. This framework is generally encountered when a limited information on the vehicle surroundings is available, such in the case of a car vehicle moving along an unknown road or an autonomous robot moving inside an environment with strong dynamics characteristics. Obstacle avoidance is generally handled through an opportune choice of the goal point and of the final robot orientation: if a collision is detected, a different target point is selected.

This work was partially supported by the University of Parma in the context of a FIL project

The authors are with the Dip. di Ing. dell’Informazione, University of Parma, I-43100 Parma, Italy, Tel. +39 0521 905752, Fax. +39 0521 905723, Email: {guarino,gerelli}@ce.unipr.it

In a motion generation context, path geometric characteristics assume a relevant role. Several path primitives, which generate continuous curvature paths, were proposed in the past: clothoids, cubic spirals [6], polar polynomials [7], intrinsic splines [8], etc.. Recently, the attention has been focused on planning primitives whose curvature is continuously differentiable [9]. Paths which possess this characteristic are named G^3 -paths. G^3 -continuity is essential especially for unicycle-like robots: in [10] it has been shown that, in order to generate continuously differentiable control signals, it is necessary to plan G^3 -paths. This requirement is not strictly necessary in the case of other autonomous vehicles, however the use of paths whose curvature is continuously differentiable leads to the generation of smooth command signals, which is, undoubtedly, a positive characteristic.

In [11], a new planning primitive, named η^3 -splines, has been proposed for the generation of G^3 -paths. η^3 -splines are planned by means of closed form expressions and always fulfill any arbitrarily assigned set of interpolating conditions. An important advantage of η^3 -splines is represented by the possibility of refining their shape, still satisfying the assigned interpolating conditions, by acting on a set of six free parameters. Such a possibility can be used, for example, for the generation of curves which satisfy appropriate optimality criteria. This property represents an important advantage of η^3 -splines but, on the other hand, poses the problem of their optimal synthesis. Since a local path generation is considered, the shaping problem must be solved online by means of an efficient procedure. This paper proposes a solution for the optimal planning of η^3 -splines which does not require the explicit online solution of an optimization problem.

In §II, the G^3 -interpolation problem is formalized (*Problem 1*) and the closed form expressions (η^3 -splines) proposed in [11] for its solution are recalled. The optimal shaping problem (*Problem 2*), which represents the key point of this paper, is formulated in the same section. The proposed solution is described in §III, and a path planning test case is presented in §IV. Final conclusions are drawn in §V.

II. PROBLEM FORMULATION

A curve in the Cartesian planar space can be described by means of the function

$$\begin{aligned} \mathbf{p} : [u_0, u_1] &\rightarrow \mathbb{R}^2 \\ u &\rightarrow \mathbf{p}(u) = [\alpha(u) \beta(u)]^T, \end{aligned}$$

where $[u_0, u_1]$ is a real closed interval. The associated “path” is the image of $[u_0, u_1]$ under the vectorial function $\mathbf{p}(u)$, i.e., $\mathbf{p}([u_0, u_1])$. We say that $\mathbf{p}(u)$ is a regular curve if $\dot{\mathbf{p}}(u)$ is piecewise continuous, i.e., $\dot{\mathbf{p}}(u) \in C_p([u_0, u_1])$, and

$\dot{\mathbf{p}}(u) \neq 0, \forall u \in [u_0, u_1]$. The arc length or, equivalently, the curvilinear coordinate measured along $\mathbf{p}(u)$, denoted by s , can be evaluated by means of the function

$$\begin{aligned} f: [u_0, u_1] &\rightarrow \mathbb{R} \\ u &\rightarrow s = \int_{u_0}^u \|\dot{\mathbf{p}}(\xi)\| d\xi \end{aligned}$$

where $\|\cdot\|$ denotes the Euclidean norm.

Associated with any point of a regular curve there is a tangent vector $\theta(u)$ measured with respect to the coordinate x -axis, a scalar curvature $\kappa(u)$, and a curvature derivative $\dot{\kappa}(u) := \frac{d\kappa}{ds}(u)$. If $\theta(u)$, $\kappa(u)$, are continuous functions over $[u_0, u_1]$, then $\mathbf{p}(u)$ is a G^2 -curve, i.e., it has a second order geometric continuity. If also $\dot{\kappa}(u)$ is continuous over $[u_0, u_1]$, then $\mathbf{p}(u)$ has a third order geometric continuity and is indicated as a G^3 -curve.

In order to control unicycle-like robots by means of continuously differentiable control signals, it is necessary to plan G^3 -curves [10]. A composite G^3 -path can be generated by combining several G^3 -curves if it is possible to assign tangents, curvatures, and curvature derivatives at the extreme points of each of them. This consideration generated the following interpolation problem

Problem 1: Assume that two points $\mathbf{p}_A := [x_A \ y_A]^T$ and $\mathbf{p}_B := [x_B \ y_B]^T$ have been assigned in the Cartesian space. Generate a G^3 -curve $\mathbf{p}(u)$ between \mathbf{p}_A and \mathbf{p}_B which fulfills given interpolating conditions on the initial and final tangent angles θ_A and θ_B , curvatures κ_A and κ_B , and curvature derivatives $\dot{\kappa}_A$ and $\dot{\kappa}_B$.

In order to solve *Problem 1*, a new planning primitive, named η^3 -splines, has been proposed in [11]. It is given by two seven order polynomial functions defined as follows

$$\mathbf{p}(u) := [\alpha(u) \ \beta(u)]^T, u \in [0, 1] \quad (1)$$

where

$$\alpha(u) := \alpha_0 + \alpha_1 u + \alpha_2 u^2 + \alpha_3 u^3 + \alpha_4 u^4 + \alpha_5 u^5 + \alpha_6 u^6 + \alpha_7 u^7; \quad (2)$$

$$\beta(u) := \beta_0 + \beta_1 u + \beta_2 u^2 + \beta_3 u^3 + \beta_4 u^4 + \beta_5 u^5 + \beta_6 u^6 + \beta_7 u^7. \quad (3)$$

In the same paper, closed form expressions were proposed in order to efficiently evaluate coefficients α_i and β_i on the basis of the interpolating conditions

$$\alpha_0 = x_A \quad (4)$$

$$\alpha_1 = \eta_1 \cos \theta_A \quad (5)$$

$$\alpha_2 = \frac{1}{2} \eta_3 \cos \theta_A - \frac{1}{2} \eta_1^2 \kappa_A \sin \theta_A \quad (6)$$

$$\alpha_3 = \frac{1}{6} \eta_5 \cos \theta_A - \frac{1}{6} (\eta_1^3 \dot{\kappa}_A + 3\eta_1 \eta_3 \kappa_A) \sin \theta_A \quad (7)$$

$$\begin{aligned} \alpha_4 = 35(x_B - x_A) &- \left(20\eta_1 + 5\eta_3 + \frac{2}{3}\eta_5\right) \cos \theta_A + \\ &+ \left(5\eta_1^2 \kappa_A + \frac{2}{3}\eta_1^3 \dot{\kappa}_A + 2\eta_1 \eta_3 \kappa_A\right) \sin \theta_A + \\ &- \left(15\eta_2 - \frac{5}{2}\eta_4 + \frac{1}{6}\eta_6\right) \cos \theta_B + \\ &- \left(\frac{5}{2}\eta_2^2 \kappa_B - \frac{1}{6}\eta_2^3 \dot{\kappa}_B - \frac{1}{2}\eta_2 \eta_4 \kappa_B\right) \sin \theta_B \end{aligned} \quad (8)$$

$$\alpha_5 = -84(x_B - x_A) + (45\eta_1 + 10\eta_3 + \eta_5) \cos \theta_A +$$

$$\begin{aligned} &- (10\eta_1^2 \kappa_A + \eta_1^3 \dot{\kappa}_A + 3\eta_1 \eta_3 \kappa_A) \sin \theta_A \\ &+ \left(39\eta_2 - 7\eta_4 + \frac{1}{2}\eta_6\right) \cos \theta_B + \\ &+ \left(7\eta_2^2 \kappa_B - \frac{1}{2}\eta_2^3 \dot{\kappa}_B - \frac{3}{2}\eta_2 \eta_4 \kappa_B\right) \sin \theta_B \end{aligned} \quad (9)$$

$$\begin{aligned} \alpha_6 = 70(x_B - x_A) &- \left(36\eta_1 + \frac{15}{2}\eta_3 + \frac{2}{3}\eta_5\right) \cos \theta_A + \\ &+ \left(\frac{15}{2}\eta_1^2 \kappa_A + \frac{2}{3}\eta_1^3 \dot{\kappa}_A + 2\eta_1 \eta_3 \kappa_A\right) \sin \theta_A \\ &- \left(34\eta_2 - \frac{13}{2}\eta_4 + \frac{1}{2}\eta_6\right) \cos \theta_B + \\ &- \left(\frac{13}{2}\eta_2^2 \kappa_B - \frac{1}{2}\eta_2^3 \dot{\kappa}_B - \frac{3}{2}\eta_2 \eta_4 \kappa_B\right) \sin \theta_B \end{aligned} \quad (10)$$

$$\begin{aligned} \alpha_7 = -20(x_B - x_A) &+ \left(10\eta_1 + 2\eta_3 + \frac{1}{6}\eta_5\right) \cos \theta_A + \\ &- \left(2\eta_1^2 \kappa_A + \frac{1}{6}\eta_1^3 \dot{\kappa}_A + \frac{1}{2}\eta_1 \eta_3 \kappa_A\right) \sin \theta_A + \\ &+ \left(10\eta_2 - 2\eta_4 + \frac{1}{6}\eta_6\right) \cos \theta_B + \\ &+ \left(2\eta_2^2 \kappa_B - \frac{1}{6}\eta_2^3 \dot{\kappa}_B - \frac{1}{2}\eta_2 \eta_4 \kappa_B\right) \sin \theta_B \end{aligned} \quad (11)$$

$$\beta_0 = y_A \quad (12)$$

$$\beta_1 = \eta_1 \sin \theta_A \quad (13)$$

$$\beta_2 = \frac{1}{2} \eta_3 \sin \theta_A + \frac{1}{2} \eta_1^2 \kappa_A \cos \theta_A \quad (14)$$

$$\beta_3 = \frac{1}{6} \eta_5 \sin \theta_A + \frac{1}{6} (\eta_1^3 \dot{\kappa}_A + 3\eta_1 \eta_3 \kappa_A) \cos \theta_A \quad (15)$$

$$\begin{aligned} \beta_4 = 35(y_B - y_A) &- \left(20\eta_1 + 5\eta_3 + \frac{2}{3}\eta_5\right) \sin \theta_A + \\ &- \left(5\eta_1^2 \kappa_A + \frac{2}{3}\eta_1^3 \dot{\kappa}_A + 2\eta_1 \eta_3 \kappa_A\right) \cos \theta_A + \\ &- \left(15\eta_2 - \frac{5}{2}\eta_4 + \frac{1}{6}\eta_6\right) \sin \theta_B + \\ &+ \left(\frac{5}{2}\eta_2^2 \kappa_B - \frac{1}{6}\eta_2^3 \dot{\kappa}_B - \frac{1}{2}\eta_2 \eta_4 \kappa_B\right) \cos \theta_B \end{aligned} \quad (16)$$

$$\begin{aligned} \beta_5 = -84(y_B - y_A) &+ (45\eta_1 + 10\eta_3 + \eta_5) \sin \theta_A + \\ &+ (10\eta_1^2 \kappa_A + \eta_1^3 \dot{\kappa}_A + 3\eta_1 \eta_3 \kappa_A) \cos \theta_A + \\ &+ \left(39\eta_2 - 7\eta_4 + \frac{1}{2}\eta_6\right) \sin \theta_B + \\ &- \left(7\eta_2^2 \kappa_B - \frac{1}{2}\eta_2^3 \dot{\kappa}_B - \frac{3}{2}\eta_2 \eta_4 \kappa_B\right) \cos \theta_B \end{aligned} \quad (17)$$

$$\begin{aligned} \beta_6 = 70(y_B - y_A) &- \left(36\eta_1 + \frac{15}{2}\eta_3 + \frac{2}{3}\eta_5\right) \sin \theta_A + \\ &- \left(\frac{15}{2}\eta_1^2 \kappa_A + \frac{2}{3}\eta_1^3 \dot{\kappa}_A + 2\eta_1 \eta_3 \kappa_A\right) \cos \theta_A + \\ &- \left(34\eta_2 - \frac{13}{2}\eta_4 + \frac{1}{2}\eta_6\right) \sin \theta_B + \\ &+ \left(\frac{13}{2}\eta_2^2 \kappa_B - \frac{1}{2}\eta_2^3 \dot{\kappa}_B - \frac{3}{2}\eta_2 \eta_4 \kappa_B\right) \cos \theta_B \end{aligned} \quad (18)$$

$$\beta_7 = -20(y_B - y_A) + \left(10\eta_1 + 2\eta_3 + \frac{1}{6}\eta_5\right) \sin \theta_A +$$

$$\begin{aligned}
& + \left(2\eta_1^2 \kappa_A + \frac{1}{6} \eta_1^3 \dot{\kappa}_A + \frac{1}{2} \eta_1 \eta_3 \kappa_A \right) \cos \theta_A + \\
& + \left(10\eta_2 - 2\eta_4 + \frac{1}{6} \eta_6 \right) \sin \theta_B + \\
& - \left(2\eta_2^2 \kappa_B - \frac{1}{6} \eta_2^3 \dot{\kappa}_B - \frac{1}{2} \eta_2 \eta_4 \kappa_B \right) \cos \theta_B \quad (19)
\end{aligned}$$

From a rapid inspection of (4)–(19), it is possible to observe their dependence on the assigned interpolating conditions $x_A, y_A, x_B, y_B, \theta_A, \theta_B, \kappa_A, \kappa_B, \dot{\kappa}_A$, and $\dot{\kappa}_B$ and on a set of six real parameters η_i . Such parameters, which give their name to the planning primitive, can be packed into a single vector $\boldsymbol{\eta} := [\eta_1 \ \eta_2 \ \eta_3 \ \eta_4 \ \eta_5 \ \eta_6]^T \in \mathcal{H} \subset (\mathbb{R}^+)^2 \times \mathbb{R}^4$.

Among the other characteristics of the $\boldsymbol{\eta}^3$ -splines, one, in particular, needs to be mentioned: $\boldsymbol{\eta}^3$ -splines always fulfill boundary conditions independently form the choice of $\boldsymbol{\eta}$. Consequently, vector $\boldsymbol{\eta}$ can be used to shape the curve interior points. This is an important feature of $\boldsymbol{\eta}^3$ -splines since it introduces flexibility in their design. On the other hand, it forces to find an appropriate method for the selection of $\boldsymbol{\eta}$. Several choices are possible. For example, in a motion planning context, $\boldsymbol{\eta}$ could be used to avoid obstacles. In a motion generation context, like that considered in this work, $\boldsymbol{\eta}$ can be used to fulfill an appropriate optimality criterion.

The control strategy developed in [10], [12] aims at generating smooth robot movements. The path shape has a strong impact on the robot lateral solicitations. In particular, it is well known that lateral accelerations are correlated to the path curvature. In the same way, lateral jerk depends on the curvature derivative with respect to the curvilinear coordinate s . In order to reduce lateral stresses, $\boldsymbol{\eta}$ can be selected by solving the following optimization problem

Problem 2: Given any set of interpolating conditions $x_A, y_A, x_B, y_B, \theta_A, \theta_B, \kappa_A, \kappa_B, \dot{\kappa}_A$, and $\dot{\kappa}_B$, find the optimal $\boldsymbol{\eta}^3$ -spline which solves the following semi-infinite minimax problem

$$\min_{\boldsymbol{\eta} \in \mathcal{H}} \max_{u \in [0,1]} \left\{ \left| \frac{d\kappa}{ds}(u; \boldsymbol{\eta}) \right| \right\} \quad (20)$$

subject to

$$\|\dot{\mathbf{p}}(u; \boldsymbol{\eta})\| > 0, \quad \forall u \in [0, 1]. \quad (21)$$

Constraint (21) is added to guarantee the curve regularity.

Problem (20)–(21) is strongly nonlinear and is characterized by a very large number of local minima. For this reason, it can only be solved by means of global optimization algorithms. For example, in this paper the optimal solution is gained by means of the hybrid genetic-interval algorithm proposed in [13], [14]. Unfortunately, this approach can only be adopted for off-line cases, since, owing to the problem complexity, evaluation times are normally not compatible with realtime applications. Consequently, it has been necessary to devise an efficient heuristic rule to be used when computational efficiency represents an important issue. Such heuristic procedure returns effective solutions and is characterized by an almost zero evaluation time. A first proposal for the optimal selection of $\boldsymbol{\eta}$ can be found in [11], where vector $\boldsymbol{\eta}$ was chosen by imposing $\eta_1 = \eta_2 = \|\mathbf{p}_A - \mathbf{p}_B\|$ and $\eta_3 = \eta_4 = \eta_5 = \eta_6 = 0$. In most practical cases this choice returns good results. Nevertheless, the problem is deeper

TABLE I
INTERPOLATING CONDITIONS Γ_i COMPATIBLE WITH CIRCULAR ARCS

	x_A	y_A	x_B	y_B	θ_A	θ_B	κ_A	κ_B	$\dot{\kappa}_A$	$\dot{\kappa}_B$
Γ_1	0	0	1.4142	0.5858	0	$\pi/4$	1/2	1/2	0	0
Γ_2	0	0	3.5355	1.4645	0	$\pi/4$	1/5	1/5	0	0
Γ_3	0	0	5.3033	2.1967	0	$\pi/4$	1/7.5	1/7.5	0	0
Γ_4	0	0	7.0711	2.9289	0	$\pi/4$	1/10	1/10	0	0
Γ_5	0	0	10.6066	4.3934	0	$\pi/4$	1/15	1/15	0	0
Γ_6	0	0	14.1421	5.8579	0	$\pi/4$	1/20	1/20	0	0
Γ_7	0	0	2.0000	2.0000	0	$\pi/2$	1/2	1/2	0	0
Γ_8	0	0	5.0000	5.0000	0	$\pi/2$	1/5	1/5	0	0
Γ_9	0	0	7.5000	7.5000	0	$\pi/2$	1/7.5	1/7.5	0	0
Γ_{10}	0	0	10.0000	10.0000	0	$\pi/2$	1/10	1/10	0	0
Γ_{11}	0	0	15.0000	15.0000	0	$\pi/2$	1/15	1/15	0	0
Γ_{12}	0	0	20.0000	20.0000	0	$\pi/2$	1/20	1/20	0	0

investigated in the following and a new rule, which produces better performance indexes, is provided.

III. THE HEURISTIC PROCEDURE

Let us indicate by $\boldsymbol{\Gamma} := [x_A \ y_A \ x_B \ y_B \ \theta_A \ \theta_B \ \kappa_A \ \kappa_B \ \dot{\kappa}_A \ \dot{\kappa}_B]^T \in \mathcal{G} \subset \mathbb{R}^4 \times [-\pi, \pi]^2 \times \mathbb{R}^4$ the vector containing the interpolating conditions used to plan a generic $\boldsymbol{\eta}^3$ -spline. The minimizer $\boldsymbol{\eta}^*$ of (20)–(21) necessarily depends on $\boldsymbol{\Gamma}$, so that it will be indicated in the following as $\boldsymbol{\eta}^*(\boldsymbol{\Gamma})$. In order to avoid an explicit online solution of (20)–(21) an algebraic function

$$\begin{aligned}
\hat{\boldsymbol{\eta}}: \mathcal{G} & \rightarrow \mathcal{H} \\
\boldsymbol{\Gamma} & \rightarrow \hat{\boldsymbol{\eta}}(\boldsymbol{\Gamma}),
\end{aligned}$$

which approximates $\boldsymbol{\eta}^*(\boldsymbol{\Gamma})$ at the best, needs to be estimated. Evidently, any effort must be spent to guarantee that curves obtained by means of $\hat{\boldsymbol{\eta}}(\boldsymbol{\Gamma})$ have performance indexes close to those obtained by means of $\boldsymbol{\eta}^*(\boldsymbol{\Gamma})$.

Function $\hat{\boldsymbol{\eta}}(\boldsymbol{\Gamma})$ is designed through a two steps procedure. The first step aims at devising a possible structure for $\hat{\boldsymbol{\eta}}(\boldsymbol{\Gamma})$. In particular, the structure of $\hat{\boldsymbol{\eta}}(\boldsymbol{\Gamma})$ is obtained by solving (20)–(21) for a set of appropriate interpolating conditions $\boldsymbol{\Gamma}_i$ and analyzing the corresponding solutions $\boldsymbol{\eta}^*(\boldsymbol{\Gamma}_i)$. The result of such analysis is a parametric function $\hat{\boldsymbol{\eta}}(\boldsymbol{\Gamma}; \mathbf{k})$, where $\mathbf{k} := [k_1 \ k_2 \ \dots \ k_{11}]^T \in \mathcal{X} \subset \mathbb{R}^{11}$ is a vector of real parameters used for its “tuning”. Then, in the second step, \mathbf{k} is evaluated by formulating a new optimization problem. The achieved optimal \mathbf{k} does not depend on $\boldsymbol{\Gamma}$, so that it can be used for any generic set of interpolating conditions.

A. Devising the structure of $\hat{\boldsymbol{\eta}}(\boldsymbol{\Gamma}; \mathbf{k})$

The structure of $\hat{\boldsymbol{\eta}}(\boldsymbol{\Gamma})$ must be characterized by its simplicity. To this purpose, let us consider some typical planning situations. Evidently, when $\kappa_A = \kappa_B$, the optimal solution of (20)–(21) is characterized by $\frac{d\kappa}{ds}(u; \hat{\boldsymbol{\eta}}) \simeq 0$, i.e., $\kappa(u; \hat{\boldsymbol{\eta}})$ is kept as constant as possible along the curve or, equivalently, the curve approximates at the best a circular arc. In the same way, if $\kappa_A \neq \kappa_B$, the optimal solution is characterized by a function $\kappa(u; \hat{\boldsymbol{\eta}})$ which almost linearly depends on s , so that $\frac{d\kappa}{ds}(u; \hat{\boldsymbol{\eta}})$ is almost constant and the curve approximates at the best a clothoid. Bearing in mind this idea, a set of interpolating conditions $\boldsymbol{\Gamma}_i$, compatible with arcs and clothoids, has been generated (see Tables I and II).

TABLE II
INTERPOLATING CONDITIONS Γ_i COMPATIBLE WITH CLOTHOIDS

	x_A	y_A	x_B	y_B	θ_A	θ_B	κ_A	κ_B	$\check{\kappa}_A$	$\check{\kappa}_B$
Γ_{13}	0	0	2.9511	0.7832	0	$\pi/4$	0	1/2	1.5915e-1	1.5915e-1
Γ_{14}	0	0	7.3776	1.9582	0	$\pi/4$	0	1/5	2.5465e-2	2.5465e-2
Γ_{15}	0	0	11.0664	2.9373	0	$\pi/4$	0	1/7.5	1.1318e-2	1.1318e-2
Γ_{16}	0	0	14.7552	3.9165	0	$\pi/4$	0	1/10	6.3662e-3	6.3662e-3
Γ_{17}	0	0	22.1327	5.8747	0	$\pi/4$	0	1/15	2.8294e-3	2.8294e-3
Γ_{18}	0	0	29.5104	7.8329	0	$\pi/4$	0	1/20	1.5915e-3	1.5915e-3
Γ_{19}	0	0	4.9107	2.7091	0	$\pi/2$	0	1/2	7.9577e-2	7.9577e-2
Γ_{20}	0	0	12.2769	6.7727	0	$\pi/2$	0	1/5	1.2732e-2	1.2732e-2
Γ_{21}	0	0	18.4152	10.1590	0	$\pi/2$	0	1/7.5	5.6588e-3	5.6588e-3
Γ_{22}	0	0	24.5538	13.5454	0	$\pi/2$	0	1/10	3.1831e-3	3.1831e-3
Γ_{23}	0	0	36.8305	20.3181	0	$\pi/2$	0	1/15	1.4147e-3	1.4147e-3
Γ_{24}	0	0	49.1075	27.0909	0	$\pi/2$	0	1/20	7.9577e-4	7.9577e-4

TABLE III
MINIMIZERS $\eta^*(\Gamma_i)$ FOR PROBLEM (20)–(21) WHEN INTERPOLATING CONDITIONS ARE CONGRUENT WITH CIRCULAR ARCS

	η_1, η_2	$\eta_3, -\eta_4$	η_5, η_6	$\left \frac{d\kappa^*}{ds} \right $
Γ_1	1.5656e+00	4.9170e-01	-6.6998e+00	1.3745e-03
Γ_2	3.6537e+00	1.3173e+00	-1.0960e+00	4.2403e-06
Γ_3	5.6959e+00	1.0188e+00	-3.7426e+00	1.5579e-07
Γ_4	7.6425e+00	1.4546e+00	-9.3034e+00	5.5453e-07
Γ_5	1.1565e+01	1.2535e+00	-8.9196e+00	4.6852e-08
Γ_6	1.5467e+01	1.3156e+00	-1.0510e+01	2.2694e-08
Γ_7	2.9465e+00	1.1786e+00	-8.6937e+00	5.7884e-05
Γ_8	7.4078e+00	2.0277e+00	-1.2477e+01	2.4701e-05
Γ_9	1.0618e+01	5.6298e+00	-1.5491e+01	8.2154e-07
Γ_{10}	1.5179e+01	1.6468e+00	-2.0441e+01	8.0685e-06
Γ_{11}	2.2828e+01	2.3025e+00	-3.3042e+01	3.3372e-06
Γ_{12}	2.9739e+01	8.4987e+00	-6.3444e+01	9.1094e-07

For each configuration Γ_i the optimal solution $\eta^*(\Gamma_i)$ has been found by means of the genetic-interval algorithm proposed in [13], [14]. As expected, in the case of interpolating conditions compatible with circular arcs, problem (20)–(21) converges toward solutions with $\frac{d\kappa}{ds} \simeq 0$, i.e., η^3 -splines almost perfectly emulate circular arcs, while, when interpolating conditions are compatible with clothoids, it converges toward constant values of $\frac{d\kappa}{ds}$ and η^3 -splines approximate clothoids. Moreover, in the case of circular arcs, owing to the symmetry characteristics of such curve ($\kappa_A = \kappa_B$, $\check{\kappa}_A = \check{\kappa}_B = 0$), the minimizers are characterized by $\eta_1 \simeq \eta_2$, $\eta_3 \simeq -\eta_4$, and $\eta_5 \simeq \eta_6$. Minimizers $\eta^*(\Gamma_i)$, $i=1,2,\dots,12$, corresponding to circular arcs, are reported in Table III. In the case of clothoids, the η_1 and η_2 are no more equal, but they remain close each other. The same happens for η_3 and $-\eta_4$, and for η_5 and η_6 . For example, for the clothoid whose interpolating conditions are given by Γ_{24} the obtained problem minimizer is $\eta_1 = 43.8944, \eta_2 = 44.8416, \eta_3 = 34.2107, \eta_4 = -28.1348, \eta_5 = -250.1721, \eta_6 = -253.6511$. For the sake of conciseness, the set of optimal solutions obtained for clothoids are herein not reported.

By scrutinizing optimal solutions $\eta^*(\Gamma_i)$, it has been possible to devise some correlations between them and the interpolating conditions reported in Tables I and II. Such information has been used to propose the following structure for $\hat{\eta}(\Gamma; \mathbf{k})$

$$\eta_1 = k_1 \|\mathbf{p}_A - \mathbf{p}_B\| + k_2 |\theta_B - \theta_A| + k_3 \sqrt{|\kappa_A|}, \quad (22)$$

$$\eta_2 = k_1 \|\mathbf{p}_A - \mathbf{p}_B\| + k_2 |\theta_B - \theta_A| + k_3 \sqrt{|\kappa_B|}, \quad (23)$$

$$\eta_3 = k_4 \|\mathbf{p}_A - \mathbf{p}_B\|^2 + k_5 |\theta_B - \theta_A| + k_6 \sqrt{|\kappa_A|} + k_7 \sqrt{|\check{\kappa}_A|}, \quad (24)$$

$$\eta_4 = -(k_4 \|\mathbf{p}_A - \mathbf{p}_B\|^2 + k_5 |\theta_B - \theta_A| + k_6 \sqrt{|\kappa_B|} + k_7 \sqrt{|\check{\kappa}_B|}), \quad (25)$$

$$\eta_5 = k_8 \|\mathbf{p}_A - \mathbf{p}_B\|^2 + k_9 \sqrt{|\theta_B - \theta_A|} + k_{10} |\kappa_A| + k_{11} \sqrt{|\check{\kappa}_A|}, \quad (26)$$

$$\eta_6 = k_8 \|\mathbf{p}_A - \mathbf{p}_B\|^2 + k_9 \sqrt{|\theta_B - \theta_A|} + k_{10} |\kappa_B| + k_{11} \sqrt{|\check{\kappa}_B|}, \quad (27)$$

where $\|\cdot\|$ indicates the Euclidean norm and $\mathbf{k} := [k_1 k_2 \dots k_{11}]^T \in \mathcal{X} \subset \mathbb{R}^{11}$ is a vector of real parameters. It is easily possible to verify that, when interpolating conditions are compatible with circular arcs, (22)–(27) correctly return $\eta_1 = \eta_2, \eta_3 = -\eta_4$, and $\eta_5 = \eta_6$, while different, but similar, values have to be expected in the case of clothoids. The same selection rule proposed in [11] can be obtained from (22)–(27) by imposing $\mathbf{k} = \mathbf{k}' := [1 0 0 0 0 0 0 0 0 0 0]^T$,

An initial estimate for \mathbf{k} has been found by means of a least square approach which minimizes the difference between $\eta^*(\Gamma)$ and $\hat{\eta}(\Gamma; \mathbf{k})$. Evidently, the obtained \mathbf{k} can only be used to generate a first rough estimate of $\hat{\eta}(\Gamma)$, since performance index $\frac{d\kappa}{ds}$ has not been taken into account during its evaluation. The optimal value \mathbf{k}'' obtained by means of this procedure is reported in Table IV.

B. Estimating the optimal \mathbf{k}

Starting from \mathbf{k}'' , it is possible to find a more “performing” value of \mathbf{k} . To this purpose, let us introduce the following optimization problem

$$\min_{\mathbf{k} \in \mathcal{X}} \{ \mathbf{J}(\mathbf{k}) \}, \quad (28)$$

where

$$\mathbf{J}(\mathbf{k}) := \sum_{i=1}^{24} \left[\frac{d\hat{\kappa}}{ds}(\Gamma_i; \mathbf{k}) - \left| \frac{d\kappa^*}{ds}(\Gamma_i) \right| \right]^2 \quad (29)$$

and where $\frac{d\hat{\kappa}}{ds}(\Gamma_i; \mathbf{k}) := \max_{u \in [0,1]} \left\{ \left| \frac{d\kappa}{ds}[u; \hat{\eta}(\Gamma_i; \mathbf{k})] \right| \right\}$ is the maximum curvature derivative obtained by means of $\hat{\eta}(\Gamma_i; \mathbf{k})$, while $\left| \frac{d\kappa^*}{ds}(\Gamma_i) \right|$ represents the maximum curvature derivative corresponding to optimal solutions $\eta^*(\Gamma_i)$ of problem (20)–(21). It is worth remembering that $\left| \frac{d\kappa^*}{ds}(\Gamma_i) \right|$ is equal to zero when interpolating conditions are compatible with circular arcs, while it is equal to the elements of the last column of Table II in the case of clothoids. Practically, the solution of (28) generates η^3 -splines whose curvature derivative is very close to the minimum obtainable for the considered interpolating conditions.

Problem (28) has been solved with an algorithm for the local optimization which started from \mathbf{k}'' . The cost index of the initial solution was equal to 1.3493. The algorithm has converged to solution \mathbf{k}''' shown in Table IV, with final performance index equal to 3.4140e-3.

Owing to the method used for the selection of \mathbf{k} , $\hat{\eta}(\Gamma; \mathbf{k}''')$ generates very good approximations of circular arcs and clothoids. But what happens in the case of generic interpolating conditions? In order to answer to this question let us consider the set of boundary conditions Γ_i reported in Tab. V. They have been selected by randomly

TABLE IV
POSSIBLE OPTIMAL PARAMETERIZATIONS FOR (22)–(27)

	\mathbf{k}'	\mathbf{k}''	\mathbf{k}'''
k_1	1	0,986215955980423	0,980241669523699
k_2	0	0,04694051539639	0,050820225241291
k_3	0	0,074863997949512	0,057298625402492
k_4	0	0,017994903356811	0,023979395751181
k_5	0	0,233918712355343	0,377342429899679
k_6	0	0,674868034806584	0,688893732522817
k_7	0	6,17884077781871	-6,88358352287906
k_8	0	-0,062562404082537	-0,15495114444297
k_9	0	-35,718866041005704	15,267133617910023
k_{10}	0	65,80182824188454	-50,110252330441334
k_{11}	0	54,58725230016439	75,23437020085763

TABLE V
RANDOMLY CHOSEN INTERPOLATING CONDITIONS Γ_i

	x_A	y_A	x_B	y_B	θ_A	θ_B	κ_A	κ_B	$\dot{\kappa}_A$	$\dot{\kappa}_B$
Γ_{25}	0	0	2.3768	-1.5950	0	-0.6126	-2.927e-1	-3.456e-1	-7.40e-3	3.99e-2
Γ_{26}	0	0	14.513	4.3664	0	0.8170	5.480e-2	1.240e-2	7.70e-3	-2.60e-3
Γ_{27}	0	0	8.0540	-4.9792	0	-0.6337	-1.820e-2	-6.140e-2	-3.40e-3	1.13e-2
Γ_{28}	0	0	5.5745	2.2956	0	0.7847	6.610e-2	2.920e-2	1.16e-2	6.60e-3
Γ_{29}	0	0	7.9545	3.5910	0	1.0043	-2.040e-2	6.620e-2	-1.17e-2	4.20e-3
Γ_{30}	0	0	3.1755	-3.4036	0	-1.5708	-1.690e-2	-1.367e-1	5.60e-3	8.20e-3
Γ_{31}	0	0	9.5297	2.1589	0	0.6170	6.970e-2	8.110e-2	-3.30e-3	1.26e-2
Γ_{32}	0	0	3.9384	3.5786	0	1.5708	-1.595e-1	1.771e-1	5.40e-3	-8.90e-3
Γ_{33}	0	0	11.115	-1.3665	0	-0.8165	-4.230e-2	-6.070e-2	-3.50e-3	-2.40e-3
Γ_{34}	0	0	9.1085	4.9272	0	0.6855	-6.620e-2	8.450e-2	-7.30e-3	-4.40e-3
Γ_{35}	0	0	4.1048	3.0115	0	1.4612	1.660e-2	1.268e-1	2.15e-2	-2.46e-2
Γ_{36}	0	0	3.2995	1.2793	0	0.3882	-1.256e-1	2.072e-1	7.60e-3	-2.00e-3
Γ_{37}	0	0	12.645	1.5489	0	0.5893	3.850e-2	2.040e-2	1.50e-3	1.80e-3
Γ_{38}	0	0	2.0141	-3.7572	0	-1.5708	2.048e-1	-2.100e-3	7.60e-3	7.00e-4
Γ_{39}	0	0	11.221	1.6647	0	0.8578	8.420e-2	6.200e-3	8.00e-3	-1.00e-4
Γ_{40}	0	0	3.5888	4.1907	0	1.4692	1.506e-1	1.405e-1	-1.70e-3	-5.00e-3
Γ_{41}	0	0	2.1525	-2.3190	0	-1.5326	-8.030e-2	-1.937e-1	-7.30e-3	8.00e-4
Γ_{42}	0	0	7.2631	-3.5370	0	-1.2966	-1.078e-1	-7.620e-2	-5.30e-3	1.28e-2
Γ_{43}	0	0	14.552	3.6728	0	1.2003	-7.100e-3	2.860e-2	5.90e-3	-5.80e-3
Γ_{44}	0	0	7.0008	-3.2704	0	-0.8977	1.250e-2	-5.090e-2	-1.24e-2	-1.52e-2
Γ_{45}	0	0	10.175	4.0194	0	1.0857	4.120e-2	8.500e-2	5.70e-3	9.90e-3
Γ_{46}	0	0	5.2888	-1.2936	0	-0.6500	2.750e-2	-1.668e-1	3.10e-3	1.02e-2
Γ_{47}	0	0	8.7662	3.5931	0	0.6804	-1.370e-2	6.000e-4	-4.00e-4	1.15e-2
Γ_{48}	0	0	14.745	3.1773	0	1.0826	-3.800e-2	4.960e-2	-5.90e-3	7.00e-3
Γ_{49}	0	0	13.331	3.5286	0	1.1674	5.740e-2	1.060e-2	3.90e-3	-8.80e-3
Γ_{50}	0	0	6.9433	-3.8030	0	-0.6980	-1.193e-1	-4.970e-2	7.60e-3	1.41e-2
Γ_{51}	0	0	5.8684	-2.4884	0	-0.8377	2.750e-2	-5.550e-2	5.40e-3	6.00e-4
Γ_{52}	0	0	9.6728	-2.4432	0	-1.0662	-7.600e-3	-4.120e-2	2.60e-3	-2.60e-3
Γ_{53}	0	0	10.181	-3.0920	0	-0.9366	-4.880e-2	-5.860e-2	-9.90e-3	-1.01e-2

choosing $x_B \in [0, 15]$, $y_B \in [-5, 5]$, $\theta_B \in [-\pi/2, \pi/2]$, $\kappa_A, \kappa_B \in [-0.4, 0.4]$, $\dot{\kappa}_A, \dot{\kappa}_B \in [-0.04, 0.04]$. Without any loss of generality, it has been supposed that $x_A = x_B = \theta_A = 0$ since, according to (22)–(27), terms η_i are evaluated on the sole basis of differences $\mathbf{p}_B - \mathbf{p}_A$ and $\theta_B - \theta_A$.

For each value of Γ_i an optimal solution $\eta^*(\Gamma_i)$ has been obtained by solving (20)–(21) with the genetic-interval algorithm, and the corresponding performance index $\left| \frac{d\kappa^*}{ds}(\Gamma_i) \right|$ has been reported in the last column of Table VI. The values of $\frac{d\hat{\kappa}}{ds}(\Gamma_i; \mathbf{k})$ corresponding to $\mathbf{k}', \mathbf{k}''$, and \mathbf{k}''' are shown in the same table. \mathbf{k}''' normally originates solutions with the smallest curvature derivatives: only in a few cases \mathbf{k}' and \mathbf{k}'' return better results. This conclusion is also confirmed by $\mathbf{J}(\mathbf{k})$. Indeed, if evaluated for $\Gamma_{25}, \dots, \Gamma_{53}$, it is equal to $\mathbf{J}(\mathbf{k}') = 2, 1596$, $\mathbf{J}(\mathbf{k}'') = 2, 6015$, and $\mathbf{J}(\mathbf{k}''') = 1, 2217$.

TABLE VI
PERFORMANCE INDEXES $\left| \frac{d\kappa^*}{ds}(\Gamma_i) \right|$ CORRESPONDING TO THE OPTIMAL SOLUTIONS OF PROBLEM (20)–(21) COMPARED WITH THE PERFORMANCE INDEXES $\frac{d\hat{\kappa}}{ds}(\Gamma_i; \mathbf{k})$ OBTAINED WITH $\mathbf{k}', \mathbf{k}''$, AND \mathbf{k}'''

	$\frac{d\hat{\kappa}}{ds}(\Gamma_i; \mathbf{k}')$	$\frac{d\hat{\kappa}}{ds}(\Gamma_i; \mathbf{k}'')$	$\frac{d\hat{\kappa}}{ds}(\Gamma_i; \mathbf{k}''')$	$\frac{d\kappa^*}{ds}(\Gamma_i)$
Γ_{25}	1,6614e+0	2,0482e+0	1,7121e+0	1,5218e+0
Γ_{26}	4,3600e-2	4,2000e-2	4,0048e-2	3,2000e-2
Γ_{27}	1,6120e-1	1,6170e-1	1,5295e-1	1,1900e-1
Γ_{28}	1,1030e-1	1,1250e-1	9,9999e-2	7,4600e-2
Γ_{29}	7,3300e-2	7,3000e-2	6,6889e-2	4,9800e-2
Γ_{30}	5,8700e-1	6,2100e-1	4,8427e-1	2,2150e-1
Γ_{31}	4,0400e-2	4,2100e-2	4,2306e-2	3,4600e-2
Γ_{32}	5,9950e-1	5,8860e-1	5,2845e-1	2,0280e-1
Γ_{33}	1,0900e-1	1,0740e-1	1,0230e-1	8,0900e-2
Γ_{34}	1,7090e-1	1,6760e-1	1,6259e-1	1,1250e-1
Γ_{35}	3,3570e-1	3,2070e-1	2,7439e-1	1,4960e-1
Γ_{36}	1,1900e+0	1,1475e+0	1,1530e+0	8,1180e-1
Γ_{37}	6,1300e-2	6,0000e-2	5,7552e-2	4,9000e-2
Γ_{38}	1,8827e+0	1,9283e+0	1,6539e+0	8,3570e-1
Γ_{39}	1,6620e-1	1,6950e-1	1,5701e-1	1,0800e-1
Γ_{40}	3,1410e-1	3,2620e-1	2,5673e-1	1,5070e-1
Γ_{41}	1,1666e+0	1,2342e+0	8,6751e-1	4,5200e-1
Γ_{42}	2,0240e-1	2,0070e-1	1,8270e-1	1,1610e-1
Γ_{43}	9,1200e-2	8,7900e-2	8,3922e-2	4,1800e-2
Γ_{44}	9,8200e-2	9,7400e-2	9,0178e-2	6,6500e-2
Γ_{45}	6,1100e-2	5,8900e-2	5,4736e-2	3,9700e-2
Γ_{46}	1,0850e-1	1,1140e-1	1,0061e-1	7,9400e-2
Γ_{47}	7,2700e-2	7,3400e-2	6,8042e-2	5,4400e-2
Γ_{48}	6,1000e-2	5,7700e-2	5,5572e-2	3,5300e-2
Γ_{49}	1,3200e-1	1,2990e-1	1,2408e-1	6,9300e-2
Γ_{50}	8,3600e-2	8,6700e-2	8,6923e-2	6,5400e-2
Γ_{51}	1,5010e-1	1,5550e-1	1,3716e-1	1,0230e-1
Γ_{52}	1,6360e-1	1,6380e-1	1,5164e-1	8,6300e-2
Γ_{53}	8,3800e-2	8,1400e-2	7,7415e-2	5,7400e-2

IV. AN APPLICATION CASE

It has been earlier pointed out that η^3 -splines are suited to be used in a real time planning scenario. Consider a wheeled mobile robot moving in an unknown environment. The trajectory is updated according to sensors information. When the updating time is reached the robot evaluates its current status, i.e., $x_A, y_A, \theta_A, \kappa_A$, and $\dot{\kappa}_A$, and determines, on the basis of the sensors data, its future desired status, i.e., $x_B, y_B, \theta_B, \kappa_B$, and $\dot{\kappa}_B$. Then, it evaluates $\hat{\eta}(\Gamma, \mathbf{k})$ by means of \mathbf{k}''' (see Table IV) and (22)–(27). Finally, the η^3 -splines coefficients are obtained by means of (4)–(19). It is worth noting that these steps are computationally efficient since are based on closed form expressions. Initial tangent, curvature, and curvature derivative of each curve are continuous with respect to those of the previous one. Then, the overall composite path is G^3 -continuous. In a realistic scenario, in order to correct tracking errors or take into account changes in the surrounding environment, e.g., moving or initially undetected obstacles, each curve is normally replanned before its end is reached by the robot. For the sake of simplicity and without any loss of generality, in the example case here reported, the curve is updated only at the end of each segment. Table VII contains the list of interpolating conditions which have been used. General interpolating conditions have been considered in order to emulate a set of actual data obtained, e.g., from a visual system. The sole exceptions are represented by Γ_{56} and Γ_{58} which are compatible with a circular arc

TABLE VII
INTERPOLATING CONDITION Γ_i CHOSEN FOR THE EXAMPLE

	x_A	y_A	x_B	y_B	θ_A	θ_B	κ_A	κ_B	$\dot{\kappa}_A$	$\dot{\kappa}_B$
Γ_{54}	0	0	5.00	8.00	0	$\pi/2$	0.1	-0.025	-0.02	-0.02
Γ_{55}	5.00	8.00	10.00	14.00	$\pi/2$	$\pi/32$	-0.025	-0.1	-0.02	0
Γ_{56}	10.00	14.00	17.32	11.78	$\pi/32$	$-7\pi/32$	-0.1	-0.1	0	0
Γ_{57}	17.32	11.78	18.00	5.00	$-7\pi/32$	$-4\pi/6$	-0.1	0	0	0
Γ_{58}	18.00	5.00	16.00	1.536	$-4\pi/6$	$-4\pi/6$	0	0	0	0

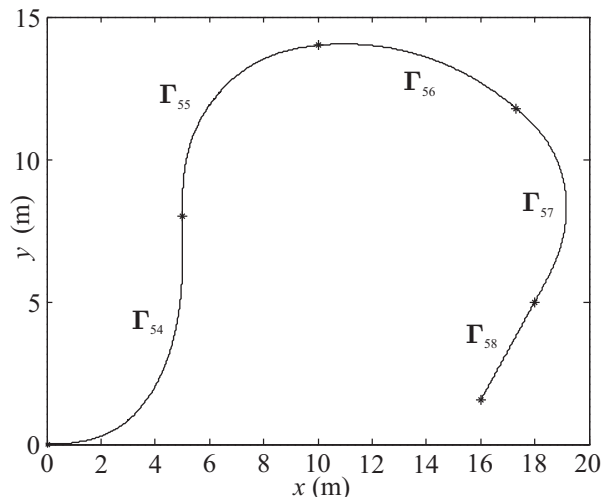


Fig. 1. The planned path.

and a linear segment respectively. The overall curve is drawn in Fig. 1. It has been obtained by using η^3 -splines, which, as known, can exactly generate linear segments when appropriate boundary conditions are assigned [11]. Fig. 2 shows the overall curvature and curvature derivative. It can be immediately noticed that they are both continuous. Moreover, they are kept small also when rough maneuvers are planned (see, e.g., Γ_{54}). Finally, it is possible to remark the very good emulation of a circular arc obtained by means of Γ_{56} : as required, the curvature is almost constant and the curvature derivative is close to zero.

V. CONCLUSIONS

Smart planar curves, suited for autonomous robots, can be generated by means of η^3 -splines. Acting on a vector η of freely selectable parameters, it is possible to shape η^3 -splines such to fulfill given optimality criteria. In this paper the generation of smooth paths has been investigated. It has been shown how, by acting on η , it is possible to generate curves with minimum curvature derivative. In order to avoid the execution of huge online optimizations, an heuristic method has been proposed for the selection of η . When interpolating conditions are compatible with circular arcs and clothoids, devised expressions generate curves which at the best emulate such primitives. In the case of generic interpolating conditions, the curvature derivative is very close to the actual achievable minimum.

ACKNOWLEDGEMENTS

The authors wish to acknowledge Eng. Paolo Baratti for the support given to this work.

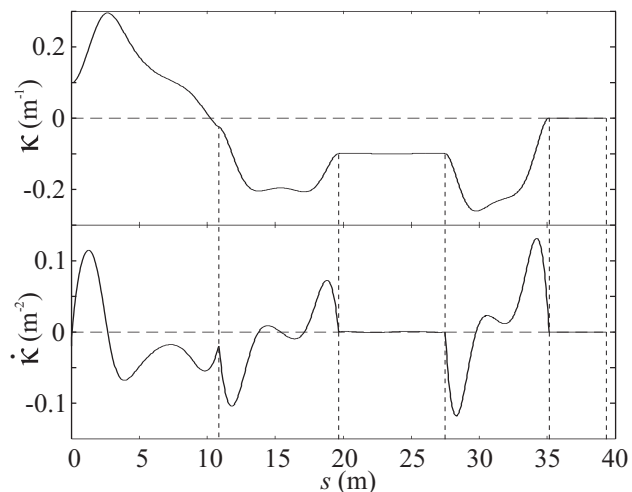


Fig. 2. The curvature and its derivative expressed with respect to the curve length s .

REFERENCES

- [1] L. Dubins, "On curves of minimal length with a constraint on average curvature and with prescribed initial and terminal positions and tangents," *American Journal of Mathematics*, vol. 79, pp. 497–517, 1957.
- [2] J. Reeds and R. Shepp, "Optimal paths for a car that goes both forward and backward," *Pacific Journal of Mathematics*, vol. 145, no. 2, pp. 367–393, 1990.
- [3] J.-D. Boissonnat, A. Cérézo, and J. Leblond, "Shortest paths of bounded curvature in the plane," in *Proc. of the 1992 IEEE Int. Conf. on Robotics and Automation*, Nice, France, May 1992, pp. 2315–2320.
- [4] P. Souères and J.-P. Laumond, "Shortest paths synthesis for a car-like robot," *IEEE Transaction on Automatic Control*, vol. 41, no. 5, pp. 672–688, May 1996.
- [5] T. Fraichard and A. Scheuer, "From Reeds and Shepp's to continuous-curvature paths," *IEEE Trans. on Robotics*, vol. 20, no. 6, pp. 1025–1035, Dec. 2004.
- [6] Y. Kanayama and B. Hartman, "Smooth local path planning for autonomous vehicles," in *Proc. of the IEEE Int. Conf. on Robotics and Automation, ICRA89*, vol. 3, Scottsdale, AZ (US), May 1989, pp. 1265–1270.
- [7] W. Nelson, "Continuous-curvature paths for autonomous vehicles," in *Proc. of the IEEE Conf. on Robotics and Automation*, vol. 3, Scottsdale, AZ, May 1989, pp. 1260–1264.
- [8] H. Delingette, M. Hébert, and K. Ikeuchi, "Trajectory generation with curvature constraint based on energy minimization," in *Proc. of the IEEE-RSJ Int. Conf. on Intelligent Robots and Systems*, Osaka, Japan, November 1991, pp. 206–211.
- [9] J. Reuter, "Mobile robots trajectories with continuously differentiable curvature: an optimal control approach," in *Proc. of the 1998 IEEE/RSJ Int. Conf. on Intelligent Robots and Systems*, vol. 1, Victoria, B.C., Canada, Oct. 1998, pp. 38–43.
- [10] C. Guarino Lo Bianco, A. Piazzzi, and M. Romano, "Smooth motion generation for unicycle mobile robots via dynamic path inversion," *IEEE Trans. on Robotics*, vol. 20, no. 5, pp. 884–891, Oct. 2004.
- [11] A. Piazzzi, M. Romano, and C. Guarino Lo Bianco, "G³-splines for the path planning of wheeled mobile robots," in *Proc. of the 2003 European Control Conference, ECC 2003*, Cambridge, UK, September 2003.
- [12] C. Guarino Lo Bianco, "Optimal velocity planning for autonomous vehicles under kinematic constraints," in *8th Int. IFAC Symp. on Robot Control, SYROCO 2006*, Bologna, Italy, Sept. 2006.
- [13] C. Guarino Lo Bianco and A. Piazzzi, "A hybrid genetic/interval algorithm for semi-infinite optimization," in *Proc. of the 35th Conf. on Decision and Control*, Kobe, Japan, December 1996, pp. 2136–2138.
- [14] —, "A hybrid algorithm for infinitely constrained optimization," *Int. J. of Systems Science*, vol. 32, no. 1, pp. 91–102, January 2001.